Membrane Topology of a 14-mer Model Amphipathic Peptide: A Solid-State NMR Spectroscopy Study†

Marise Ouellet, Jean-Daniel Doucet, Normand Voyer, and Michèle Auger*

Département de Chimie, Centre de Recherche sur la Fonction, la Structure et l'Ingénierie des Protéines, Centre de Recherche en Sciences et Ingénierie des Macromolécules, Université Laval, Québec, Québec, Canada G1K 7P4

Received September 28, 2006; Revised Manuscript Received April 4, 2007

ABSTRACT: We have investigated the interaction between a synthetic amphipathic 14-mer peptide and model membranes by solid-state NMR. The 14-mer peptide is composed of leucines and phenylalanines modified by the addition of crown ethers and forms a helical amphipathic structure in solution and bound to lipid membranes. To shed light on its membrane topology, ^{31}P, ^{2}H, ^{15}N solid-state NMR experiments have been performed on the 14-mer peptide in interaction with mechanically oriented bilayers of dilauroylphosphatidylcholine (DLPC), dimyristoylphosphatidylcholine (DMPC), and dipalmitoylphosphatidylcholine (DPPC). The ^{31}P, ^{2}H, and ^{15}N NMR results indicate that the 14-mer peptide remains at the surface of the DLPC, DMPC, and DPPC bilayers stacked between glass plates and perturbs the lipid orientation relative to the magnetic field direction. Its membrane topology is similar in DLPC and DMPC bilayers, whereas the peptide seems to be more deeply inserted in DPPC bilayers, as revealed by the greater orientational and motional disorder of the DPPC lipid headgroup and acyl chains. $^{15}N\{^{31}P\}$ rotational echo double resonance experiments have also been used to measure the intermolecular dipole−dipole interaction between the 14-mer peptide and the phospholipid headgroup of DMPC multilamellar vesicles, and the results indicate that the 14-mer peptide is in contact with the polar region of the DMPC lipids. On the basis of these studies, the mechanism of membrane perturbation of the 14-mer peptide is associated to the induction of a positive curvature strain induced by the peptide lying on the bilayer surface and seems to be independent of the bilayer hydrophobic thickness.

In recent years, there has been a growing interest in studying membrane-active peptides since they represent a potential alternative to ineffective antibiotics (*1*). Most of the natural occurring antimicrobial peptides are short, diversified in their amino acid composition, cationic, amphipathic, and can adopt different structures in interaction with membranes (*2*, *3*). Their membrane activity seems to be modulated both by the structural parameters of the peptides, such as helicity, charge, hydrophobicity, and the lipidic composition, and by the physical state of the membranes (*4*). As reported by Hancock et al., Jenssen et al., and Marr et al., several variants of cationic antimicrobial peptides are currently being investigated and present varied successes in clinical tests (*5*−*7*). Even if the development of antimicrobial peptides for clinical applications remains challenging, these agents possess advantages that overcome limitations of conventional antibiotics.

The antibacterial activity of natural membrane-active peptides has been extensively studied, and the readers are referred to the paper of Strandberg et al. (*8*) for a detailed list of synthetic and natural antimicrobial peptides studied by solid-state NMR.[1] Besides their antibacterial activity, some membrane-active peptides like melittin, indolicidin, and cecropin-like human LL-37 show important cytotoxic properties. As reported by Hancock et al., it is very difficult to predict the hemolytic activity of some antibacterial peptides (*9*), and it is essential for the design of novel synthetic antibacterial agents to better understand the types of interactions involved both in the antibacterial and in the hemolytic activities of such agents. However, the ways by which membrane-active peptides perturb lipid bilayers are not well understood, and many researches have relied on synthetic model peptides to shed light on the mode of membrane perturbation and on the structural features that drive these mechanisms (*10*−*12*). General modes of action are reported in the literature, namely, the barrel-stave, the carpet-like, the

† This work was supported by the Natural Science and Engineering Research Council (NSERC) of Canada, by the Fonds Québécois de la Recherche sur la Nature et les Technologies (FQRNT), by the Centre de Recherche sur la Structure, la Fonction et l'Ingénierie des Protéines (CREFSIP), and by the Centre de Recherche en Sciences et Ingénierie des Macromolécules (CERSIM). M.O. and J.-D.D. also wish to thank NSERC for the award of postgraduate and undergraduate scholarships, respectively.

* Address correspondence to this author. Tel: 418-656-3393. Fax: 418-656-7916. E-mail: michele.auger@chm.ulaval.ca.

[1] Abbreviations: BOC, *tert*-butyloxycarbonyl; CP, cross-polarization; CSA, chemical shift anisotropy; DLPC, dilauroylphosphatidylcholine; DMF, *N*,*N*-dimethyl sulfoxide; DMPC, dimyristoylphosphatidylcholine; DOTAP, 1,2-dioleoyl-3-(trimethylammonio)propane; DPPC, dipalmitoylphosphatidylcholine; DVB, divinylbenzene; FWHM, full width at half-maximum; HPLC, high-performance liquid chromatography; LPC, lysophosphatidylcholine; MAS, magic-angle spinning; MLVs, multilamellar vesicles; NMR, nuclear magnetic resonance; PC, phosphatidylcholine; POPC, 1-palmitoyl-2-oleoylphosphatidylcholine; POPE, 1-palmitoyl-2-oleoylphosphatidylethanolamine; POPG, 1-palmitoyl-2-oleoylphosphatidylglycerol; POPS, 1-palmitoyl-2-oleoylphosphatidylserine; REDOR, rotational echo double resonance; TPPM, two pulse phase modulation.

10.1021/bi0620151 CCC: $37.00
Published on Web 05/08/2007

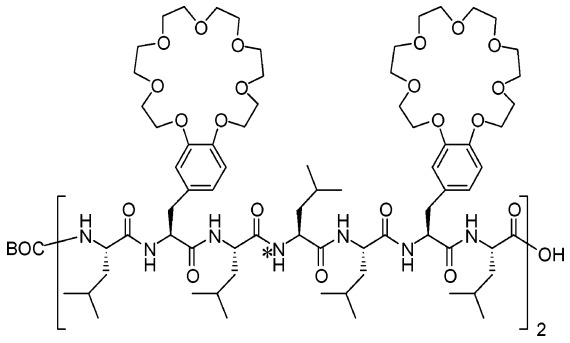

FIGURE 1: Monoprotected 14-mer peptide used in the present study. The ^{15}N-labeled leucine residue marked by an asterisk is located in the first heptamer at position 4.

toroidal, and the detergent-like models (*13*−*15*). A detailed examination of these mechanisms seems to reveal a correlation between the peptide membrane topology and the membrane disturbing effect.

Many research groups have concentrated their efforts on the design of synthetic model peptides with varying structural parameters such as membrane-anchor extremities, pH-sensitive side chains, or different hydrophobic lengths. In order to better understand the type of interactions involved in the hemolytic activity of membrane-active peptides, we have designed a synthetic helical amphipathic peptide that is an oligomer of a repeating unit of five leucine residues and two synthetic 21-crown-7-phenylalanines appropriately positioned so that the hydrophilic crown ethers align on one side of the hydrophobic helical axis to form a neutral amphipathic 14-mer peptide (Figure 1). Neutral peptides are rarely studied because antimicrobial activity is known to increase with cationic charge (*16*). However, from a mechanistic perspective, an uncharged peptide with membrane disruption activity allows studies mainly of the effect of hydrophobic forces, which seem to dominate the hemolytic activity of membrane-active peptides, on the interaction with lipids without the influence of strong electrostatic forces. The 14-mer peptide constitutes a very good model to study the interaction between lipids and membrane-active peptides since it is short and can be easily chemically modified.

Solid-state NMR spectroscopy allows the study of static samples that are aligned with respect to the magnetic field, and it then takes advantage of the orientational dependence of anisotropic interactions such as the chemical shift. Alternatively, the use of magic-angle sample spinning (MAS) allows the measurement of internuclear distances with relatively high accuracy (*17*−*19*). Many examples of solid-state NMR membrane topology studies of natural antimicrobial peptides are reported in the literature and allow a better understanding on their membrane activity. For example, results obtained for the antibiotic ionophore alamethicin support the "barrel-stave" model in a transmembrane fashion in both nonconductive and conductive states (*20*). Many members of the magainin family, such as the antimicrobial peptide PGLa and the analogue MSI-78, show an in-plane orientation that seems to be correlated to their antibacterial activity (*21*−*23*).

In the present study, we have determined by solid-state NMR spectroscopy the membrane topology of the membrane-active 14-mer peptide in lipid bilayers to obtain more information on its mode of membrane perturbation. Static experiments have been performed on mechanically oriented bilayers composed of DLPC, DMPC, and DPPC. Static ^{31}P NMR spectroscopy has first been used to obtain information on the quality of the bilayer alignment, on the lipid phase, and on the conformation of the polar headgroups upon peptide binding. Static ^{2}H NMR spectroscopy has been used to investigate the acyl chain order in DMPC and DPPC oriented bilayers upon the 14-mer peptide addition. Subsequently, ^{15}N NMR spectroscopy has been performed on mechanically aligned bilayers to obtain information on the 14-mer peptide membrane topology. Finally, a rotational echo double resonance (REDOR) experiment has been performed to obtain information on the proximity of the 14-mer peptide with the DMPC headgroups. The results strongly suggest that the 14-mer peptide lies at the bilayer surface, regardless of the bilayer thickness, and destabilizes the lipid bilayer via the induction of a positive curvature strain.

MATERIALS AND METHODS

Materials. DLPC, DMPC, and DPPC were purchased from Avanti Polar Lipids (Alabaster, AL) and used without purification. Oxime resin was prepared by a standard procedure using polystyrene beads (100−200 mesh, 1% DVB; Advanced ChemTech, Louisville, KY) (*24*). Resins with substitution levels around 0.5 mmol/g of oxime group were used. Boc-protected amino acids were purchased from Advanced ChemTech (Louisville, KY). The [^{15}N]leucine residue was purchased from Cambridge Isotope Laboratories (Andover, MA). All solvents were of reagent grade, spectrograde, or HPLC grade quality purchased commercially and used without any further purification except for DMF (degassed with N_2), dichloromethane (distilled), and diethyl ether (distilled from sodium and benzophenone). Water used throughout the studies was distilled and deionized using a Barnstead NANOpurII system (Boston, MA) with four purification columns. All other reagents were purchased from Sigma Aldrich Co. (Milwaukee, WI). Glass cover slides of 0.13−0.17 mm thickness were purchased from VWR Scientific (West Chester, PA) and cut into 10 mm × 20 mm rectangles.

Peptide Synthesis. The unlabeled and ^{15}N-labeled monoprotected 14-mer peptides were synthesized and purified according to published procedures (*25*). The N-terminal region of the 14-mer peptide is Boc-protected while the C-terminal region is deprotected. The [^{15}N]leucine residue has been incorporated into the first heptamer segment at position 4 in the amino acid sequence.

Sample Preparation. (A) Oriented Bilayers between Glass Plates. The DLPC, DMPC, and DPPC bilayers were prepared by dissolving 30 mg of phospholipids in 120 μL of chloroform, and the solution was deposited onto 18 thin cover glasses. The glass plates were allowed to dry in air for 24 h and then stacked and hydrated with deionized water in a closed chamber for at least 24 h at 70 °C. Subsequently, the plates were wrapped in Parafilm before use. This procedure yielded satisfactory alignment of the membrane, as indicated by the narrow ^{31}P resonances of the lipids (Figure 2). For the preparation of the peptide-containing bilayers, the dry peptide was codissolved with dry lipids in chloroform in a lipid/peptide molar ratio of 60:1. The following steps are the same as described above for the preparation of

pure aligned bilayers stacked between glass plates. Since the lipids found in natural membranes are in the fluid phase, the NMR spectra of mechanically oriented bilayers have been obtained at temperatures above the lipid phase transition, i.e., at 37 °C for the DLPC and DMPC bilayers and 50 °C for DPPC bilayers.

(B) Lyophilized Sample. Dry DMPC (40 mg) and the 14-mer peptide in a lipid/peptide molar ratio of 60:1 were codissolved in 180 μL of chloroform to ensure thorough mixing. The solvent was removed under nitrogen gas, followed by storage under vacuum overnight to remove all traces of organic solvent. The dry sample was hydrated with 180 μL of deionized water with 20% (w/w) lipids in water. The resulting suspension underwent at least three freeze (liquid N_2)/thaw (lipid phase transition temperature of 23 °C + 7 °C)/vortex shaking cycles to ensure the formation of multilamellar vesicles. The sample was rapidly frozen, lyophilized overnight, and then packed into a 4 mm NMR tube prior to data acquisition.

NMR Experiments. (A) Static ^{31}P, ^{2}H, and ^{15}N NMR Experiments. The static proton-decoupled ^{31}P and ^{15}N NMR spectra, and ^{2}H NMR spectra, were acquired with a Bruker Avance 300 MHz spectrometer (Bruker Canada, Milton, Ontario, Canada). The ^{31}P NMR spectra were obtained at 121.5 MHz with TPPM proton decoupling (*26*). Using 2048 data points, typically 1200 scans were acquired with a pulse length of 6 μs and a recycle delay of 4 s. The spectral width was 50 kHz, and a line broadening of 50 Hz was applied to all static ^{31}P spectra. The thin glass plates were inserted into a flat coil of a home-built solid-state NMR probe head with the glass plate normal oriented parallel to the magnetic field direction. The chemical shifts were referenced relative to external H_3PO_4, 85% (0 ppm).

The ^{2}H NMR experiments were carried out at 46.1 MHz using a quadrupolar echo sequence (*27*). The 90° pulse length was 5 μs, and the interpulse delay was 60 μs. A total of 6400 scans were acquired using 4K data points, and the recycle time was set to 500 ms. The thin glass plates were inserted into a flat coil of a home-built solid-state NMR probe head. A line broadening of 100 Hz was applied to all static ^{2}H NMR spectra.

The ^{15}N NMR spectra were obtained at 30.4 MHz using a cross-polarization (CP) pulse sequence with TPPM proton decoupling (*26*). Using 2048 data points, typically 100000 scans were acquired with a ^{1}H$-^{15}$N CP contact time of 3 ms and a recycle delay of 4 s. The spectral width was 30 kHz, and a line broadening of 300 Hz was applied to all ^{15}N oriented spectra. The chemical shifts were referenced relative to external $^{15}NH_4Cl$ (41.5 ppm) corresponding approximately to 0 ppm for liquid NH_3.

(B) REDOR Experiments. NMR spectra were acquired with a Bruker Avance 400 MHz spectrometer (Bruker Canada, Milton, Ontario, Canada). REDOR requires that two spectra be collected, one with pulses on the I channel to produce the spectrum S and one without to produce the S_0 spectrum. The ratio of the difference between the two spectra ($\Delta S = S_0 - S$) and S_0 can be related to the dipolar coupling D_{IS}, and then the internuclear distance can be easily calculated using the equation $r_{IS} = [(\epsilon_0\gamma_I\gamma_S h)/16\pi^2 D_{IS}]$, where ϵ_0 is the vacuum permeativity, γ_I and γ_S are the gyromagnetic ratios of the I and S spins, respectively, h is the Planck constant, and the dipolar coupling, D_{IS}, is in hertz (*28*). The spinning speed was 3800 Hz. The ^{1}H$-^{15}$N CP contact time was 1 ms with a matched spin-locked CP of 30.4 kHz. Spectra were obtained with a recycle delay of 3 s and ^{1}H decoupling field strength of 83.0 kHz. Spectra were processed with a 200 Hz line broadening. The phase cycling XY8 was used to compensate for errors in the flip angle, resonance offset effects, and variation in the B_1 field (*29*). The B_1 field values were 41.7 kHz for ^{31}P 180° pulses and 35.7 kHz for ^{15}N 180° pulses. The acquisition temperature was −10 °C to reduce motional averaging. The sample was placed into a 4 mm NMR tube inserted into a magic-angle spinning (MAS) probe. The chemical shifts were referenced relative to external $^{15}NH_4Cl$ (41.5 ppm) corresponding approximately to 0 ppm for liquid NH_3. Bessel function expressions in Microsoft Excel were used to simulate the $\Delta S/S_0$ versus dephasing time ($N_c T_r D$) curves, where N_c is the number of rotor cycles before data acquisition, T_r is the rotor period, and D is the dipolar coupling constant (*28*).

RESULTS AND DISCUSSION

Peptide Design. The general idea behind the design of the 14-mer peptide investigated in the present study was to use an α-helical peptidic framework made of leucines and phenylalanines modified with crown ethers. These two amino acids are known for their high propensity to induce a helical conformation to the chain, and the crown ethers are ingeniously positioned to lead to their alignment under such helical form. The polar crown ethers on one side and the hydrophobic leucine side chains on the opposite side result in an amphipathic peptide that can mimic native properties of natural membrane-active peptides. Both the peptide helical and amphipathic characters were important structural features to assess because they allow an optimal interaction with amphipathic biological membranes. Synthetic crown ethers have been used as the constituent for the polar face of the helix due to their neutral polar character and the ease by which their size can be modified, therefore allowing control on structural parameters such as the peptide amphipathic character and polar angle. More specifically, 21-crown-7 macrocyclic ethers were selected because of their low binding affinity to alkali metal ions and their more significant polar character as compared to smaller crown ethers. The conformation of the 14-mer peptide has been investigated by circular dichroism spectropolarimetry, and the results revealed that it adopts a helical conformation (*30*).

Because we are interested in defining the role played by hydrophobic interactions in the membrane perturbation by membrane-active peptides, and that the hemolytic activity is closely related to the peptide hydrophobic character, we have studied the 14-mer peptide in its uncharged form (*4*). The membrane perturbing activity of the 14-mer peptide has previously been studied by fluorescence and ^{23}Na NMR spectroscopies and revealed that the 14-mer peptide promotes the rapid release of calcein and Na^+ from vesicles and hemoglobin from erythrocytes (*30*). Preliminary studies have been performed to evaluate the antibacterial activity of the 14-mer peptide in *Escherichia coli* Gram-negative bacteria by the use of the broth dilution method from which the minimal inhibitory concentration is calculated (unpublished results). The 14-mer peptide was tested at concentrations of 10, 1, 0.1, and 0.01 μM, and no growth inhibition was observed. As expected from its composition and conforma-

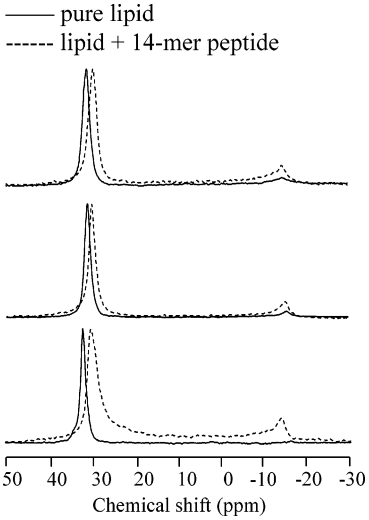

FIGURE 2: ^{31}P NMR spectra of mechanically oriented lipid bilayers of DLPC (top row) and DMPC (middle row) at 37 °C and DPPC (bottom row) at 50 °C in the absence and presence of the 14-mer peptide at a lipid/peptide molar ratio of 60:1.

tion, the 14-mer peptide exhibits a cytolytic activity on human red blood cells with a minimal concentration of 4 μM. These studies indicate a high membrane activity for the 14-mer peptide and, more specifically, a hemolytic activity. The 14-mer peptide therefore constitutes a good model to study the way by which antibacterial peptides with hemolytic activity perturb the bilayer integrity. We have also performed ^{31}P and ^{2}H solid-state NMR experiments on unoriented zwitterionic and anionic vesicles, and the results showed that the 14-mer peptide affects the conformation of the lipid polar headgroup and weakly orders the lipid acyl chains (*31*), suggesting an in-plane orientation of the 14-mer peptide.

Solid-State NMR Spectroscopy. (A) Phosphorus-31 NMR. Since the phospholipid headgroup contains a phosphorus-31 atom with a 100% natural isotopic abundance, ^{31}P NMR is a powerful technique to monitor changes occurring in the polar region of the bilayer (*32*−*34*). We have used ^{31}P NMR spectroscopy to investigate changes occurring in the headgroup region of mechanically aligned bilayers of DLPC, DMPC, and DPPC upon the addition of the 14-mer peptide. The choice of lipids with different acyl chain lengths was aimed to determine whether the bilayer thickness can affect the membrane topology of the 14-mer peptide. More specifically, static ^{31}P solid-state NMR spectra provide information on the conformation of the polar headgroup and on the quality of the alignment of phospholipid bilayers by analyzing changes in the chemical shift (δ, ppm) and in the full width at half-maximum (fwhm, ppm) of the resonance and in the chemical shift anisotropy (CSA, ppm) throughout the entire spectrum.

We have first investigated the effect of the 14-mer peptide on zwitterionic bilayers of different acyl chain lengths, namely, DLPC (19.8 Å), DMPC (24.4 Å), and DPPC (26.6 Å) bilayers (*35*). These average chain length values are reported by Petrache et al. (*35*) for lipids in the liquid-crystalline state at temperatures of 30 °C for DLPC and DMPC and 50 °C for DPPC. The ^{31}P NMR static spectra and related spectral parameters of pure and peptide-containing lipid systems are displayed in Figure 2 and Table 1. The spectra of the pure lipid systems are characteristic of well-

Table 1: ^{31}P NMR Spectral Parameters for DLPC, DMPC, and DPPC Bilayers in the Absence and Presence of the 14-mer Peptide at a Lipid/Peptide Molar Ratio of 60:1

	δ (ppm)			fwhm (ppm)		% alignment	
	pure	14-mer	S_2	pure	14-mer	pure	14-mer
DLPC	31.2	29.7	0.95	1.9	2.3	72	57
DMPC	31.1	30.1	0.97	1.7	1.9	81	64
DPPC	32.0	30.1	0.94	1.5	3.6	99	63

aligned bilayers in the fluid phase with the bilayer normal parallel to the external magnetic field B_0, with a minimal contribution of 90° aligned lipids with acyl chains perpendicular to the B_0 direction. As reported in Table 1, a single and sharp resonance is observed for DLPC (DMPC, DPPC) at 31.2 ppm (31.1 ppm, 32.0 ppm), with a full width at half-maximum (fwhm) of 1.9 ppm (1.7 ppm, 1.5 ppm). We evaluate the proportion of aligned versus nonaligned lipids by the ratio of the spectral area of the single resonance (corresponding to lipids oriented parallel to the magnetic field direction) over the entire spectral area, expressed in percentage (*36*). For DLPC, DMPC, and DPPC systems, we obtain a percentage of alignment of 72%, 81%, and 99%, respectively.

The ^{31}P NMR spectra of the DLPC bilayers with and without the 14-mer peptide are presented in Figure 2 (top row). The ^{31}P NMR spectrum of the pure system shows one single intense resonance with δ and fwhm of 31.2 and 1.9 ppm. Upon the 14-mer peptide binding, there is a decrease in the CSA reflected by the resonance being shifted by 1.5 ppm and broadened by 0.4 ppm. There is also the appearance of a small resonance at −14.6 ppm and an increase of the spectral intensity throughout the powder pattern, i.e., between 29.7 and −14.6 ppm. The lipid/peptide system shows a degree of 0° alignment of 57% compared to 72% for pure DLPC bilayers. In the pure DMPC bilayers [Figure 2 (middle row)], a single resonance appears at 31.1 ppm with a line width of 1.7 ppm. As shown on the NMR spectrum, the decrease in the CSA upon the 14-mer peptide binding is reflected by a resonance shift of 1.0 ppm and a broadening of the resonance by 0.2 ppm. A new component characteristic of 90° aligned lipids also appears at −15.3 ppm. As in the DLPC/14-mer system, the spectral intensity between 30.1 and −15.3 ppm is slightly increased upon peptide addition, and the system shows a degree of 0° alignment of 64% compared to 81% for pure DMPC bilayers. In pure DPPC bilayers [Figure 2 (bottom row)], a single resonance is observed at 32.0 ppm with a line width of 1.5 ppm. Upon the 14-mer peptide addition to the DPPC bilayers, the decrease in the CSA is reflected by a resonance shift of 1.9 ppm and a broadening of 2.1 ppm, and the system shows a change in the degree of alignment, which is evaluated at 99% for the pure system and at 63% for the peptide-containing bilayers. As observed for the DLPC and DMPC bilayers, a new component characteristic of 90° aligned lipids appears at −13.8 ppm with an increase of the spectral intensity throughout the powder pattern. By analyzing the three lipid systems, it seems that the 14-mer peptide perturbs the conformation of the lipid polar headgroup in a similar manner, but subtle changes are observed on the NMR spectra of the three lipid systems. The DPPC lipids have longer acyl chains than DLPC and DMPC lipids and then stronger van der Waals forces between adjacent DPPC lipids (*35*). These

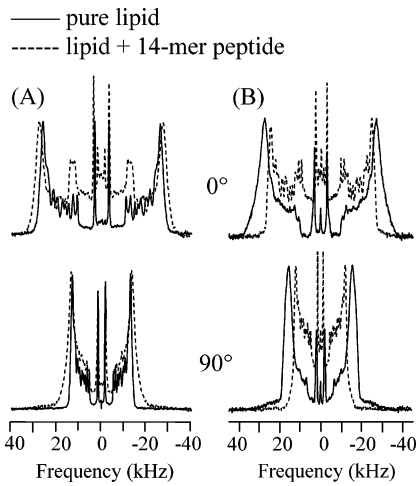

FIGURE 3: ^{2}H NMR spectra of mechanically oriented lipid bilayers of (A) DMPC at 37 °C and of (B) DPPC at 50 °C with the bilayer normal parallel (top row) and perpendicular (bottom row) to the magnetic field direction in the absence and presence of the 14-mer peptide at a lipid/peptide molar ratio of 60:1.

forces result in an overall stabilization of the bilayer that is reflected on the ^{2}H NMR spectrum of DPPC by the larger quadrupolar splitting (Figure 3B) and keep the headgroups closer together. On the other hand, the ^{31}P NMR spectra have been recorded at 37 °C for DLPC and DMPC bilayers, corresponding to a difference of 38 and 14 °C compared to their temperature phase transitions, respectively. For the DPPC system, however, the ^{31}P NMR spectra have been recorded at 50 °C which is only 7 °C above the phase transition. The greater effect on the conformation and/or orientation of the DPPC lipid headgroups upon the 14-mer peptide binding can be explained by the fact that the pure DPPC bilayers are more ordered than the DLPC and DMPC bilayers and then less susceptible to accommodate a membrane surface defect. The effect of the 14-mer peptide seems then to be more amplified in DPPC bilayers than in DLPC and DMPC bilayers. Picard et al. have proposed another way to quantify the effect of peptides on the chemical shift by evaluating a relative order parameter of the form:

$$S_2 = \delta/\delta_{\text{ref}} \tag{1}$$

in which δ_{ref} is the chemical shift of a reference system, such as the pure lipid system in the absence of the 14-mer peptide (*37*). As seen in Table 1, we obtain S_2 values of 0.95, 0.97, and 0.94 for DLPC, DMPC, and DPPC bilayers, respectively. These S_2 values quantify the slight perturbing effect of the 14-mer peptide on the lipid headgroup dynamics and/or orientation of the DLPC, DMPC, and DPPC bilayers.

The overall decrease in the CSA observed in DLPC, DMPC, and DPPC bilayers upon the addition of the 14-mer peptide could be explained by an interaction of the peptide at the polar headgroup of the lipids. The strategic positioning of the crown ethers at sites 2, 6, 9, and 13 makes all the crown ethers well sequestered on one side of the α-helix and confers an amphipathic nature to the 14-mer peptide. When inserted into the bilayer, the crown ethers are likely facing the aqueous phase, whereas the hydrophobic helix composed of mainly leucine residues is likely facing the hydrophobic region of the bilayer. The possible interfacial location of the 14-mer peptide could then affect the conformation of the polar headgroups of DLPC, DMPC, and DPPC bilayers. Buffy et al. also observed orientational disorder of lipids in interaction with the antimicrobial peptide RTD-1, whatever the varying lipid acyl chain length, suggesting that RTD-1 binds to the bilayer surface (*36*). Another important feature observed on the ^{31}P NMR spectra is the appearance of a broad powder pattern in DLPC, DMPC, and DPPC spectra, as depicted in Figure 2. This is reflected in the calculation of the percentage of alignment disorder as shown in Table 1. For DLPC, DMPC, and DPPC bilayers, there is a loss of parallel orientation of 15%, 17%, and 36%, respectively. It is important to mention that two distinct ^{31}P NMR experiments have been performed for each system investigated to make sure that the unoriented component observed on the ^{31}P NMR spectra originates from the membrane interaction of the 14-mer peptide and not from variability in the sample preparation. The duplicate spectra are highly reproducible and show the same trend, namely, an increase in the percentage of misalignment with an increase in the lipid acyl chain length.

Mecke et al. have reported an upfield shift of the DMPC resonance, and a broad line of low intensity, upon MSI-78 binding, an analogue of the magainin family (*23*). They attributed the shift to either a tilt of the lipid and/or a change of the lipid headgroup conformation and the powder pattern of low intensity to different orientations of the lipids. Harzer et al. have studied model peptides composed of leucine and alanine residues in interaction with POPC membranes (*12*). They have also attributed changes in the ^{31}P chemical shift and the signal intensity of nonoriented lipids to conformational and/or orientational changes at the lipid headgroup or to the phospholipids as a whole. The broadening of the 0° oriented resonance has also been observed upon the protegrin-1 binding to POPC/POPG bilayers (*38*). Mani et al. explained the asymmetric broadening of the 0° resonance by an increase in the mosaic spread of the bilayers. From ^{31}P NMR spectra, it seems that the 14-mer peptide disrupts both the dynamics and/or orientation of the polar headgroup as well as the quality of orientation of the lipids as revealed by the S_2 order parameter and the percentage of alignment values. These effects are however more pronounced for DPPC bilayers than for DLPC and DMPC bilayers.

(B) Deuterium NMR. We have investigated the effect of the 14-mer peptide on the lipid order of bilayers stacked between glass plates by measuring the quadrupolar splitting upon peptide addition. The increase (decrease) in the quadrupolar splitting ($\Delta\nu_Q$) for a C−D bond is associated to order (disorder) in the deuterated chains and is related to an order parameter S_{CD}:

$$\Delta\nu_Q = \frac{3}{4}\left(\frac{e^2qQ}{h}\right)(3\cos^2\theta - 1)S_{CD} \tag{2}$$

where e^2qQ/h is the quadrupole coupling constant for C−D bonds (∼167 kHz) and θ is the angle between the bilayer normal and B_0 (*32*).

The ^{2}H static NMR spectra and related spectral parameters of peptide-containing bilayers stacked between glass plates are shown in Figure 3 and Table 2. A lipid/peptide molar ratio of 60:1 was used, and the spectra were recorded at 37 and 50 °C for DMPC and DPPC bilayers. The spectra have

Table 2: Quadrupolar Splitting and S_{CD} Order Parameters of DMPC-d_{54} and DPPC-d_{62} for the Plateau and Methyl Regions in 0° Oriented Bilayers in the Absence and Presence of the 14-mer Peptide at a Lipid/Peptide Molar Ratio of 60:1

	$\Delta\nu_P$ (kHz)		$S_{CD(P)}$		$\Delta\nu_M$ (kHz)		$S_{CD(M)}$	
	pure	14-mer	pure	14-mer	pure	14-mer	pure	14-mer
DMPC	52.5	55.5	0.41	0.44	6.3	6.8	0.05	0.05
DPPC	55.0	49.6	0.43	0.39	6.0	5.5	0.05	0.04

been recorded at two bilayer alignments, with the bilayer normal parallel and perpendicular to the magnetic field direction. The pure DMPC [Figure 3A (top row)] and DPPC bilayers [Figure 3B (top row)] in a parallel orientation show a quadrupolar splitting $\Delta\nu_P$ of 52.5 and 55.0 kHz for the plateau region and a $\Delta\nu_M$ of 6.3 and 6.0 kHz for the terminal methyl group of the lipid acyl chains. Upon the 14-mer peptide addition to the DMPC and DPPC bilayers, two different spectral patterns are observed on the DMPC and DPPC ^{2}H NMR spectra. The first spectral feature is an increase of the $\Delta\nu_P$ of DMPC by 3.0 kHz, whereas the $\Delta\nu_P$ of DPPC is decreased by 5.4 kHz. This ordering at the plateau region of the DMPC acyl chains is reflected by an S_{CD} order parameter of 0.44 compared to the pure bilayers with an S_{CD} order parameter of 0.41. The methyl group of DMPC bilayers is not significantly affected by the 14-mer peptide. This is reflected by an unchanged S_{CD} order parameter of 0.05. The DPPC acyl chains are globally disordered upon the addition of the 14-mer peptide, with S_{CD} order parameters of 0.39 (0.04) for the plateau (methyl) region, compared to the pure DPPC bilayers with S_{CD} order parameters of 0.43 (0.05). The second spectral feature observed upon the peptide addition in both bilayers is the presence of a powder pattern at ±10 kHz. ^{2}H NMR spectra have then been acquired at the 90° orientation to determine whether this powder pattern originates from a large decrease of the maximal quadrupolar splitting for a fraction of oriented lipids or from nonoriented lipids in DMPC and DPPC bilayers. If the powder pattern at ±10 kHz originates from a large decrease of the maximal quadrupolar splitting, a powder pattern at ±5 kHz should be observed on ^{2}H NMR spectra acquired at the 90° orientation. Mani et al. and Yamaguchi et al., who have studied the antimicrobial peptide protegrin-1, observed a similar behavior in POPC and POPC/POPG bilayers in both bilayer orientations at various lipid/peptide molar ratios (*39*, *40*). They attributed the signals to nonoriented lipids that deviate from the initial parallel orientation before the peptide addition. As observed in the ^{31}P NMR spectra of DMPC and DPPC bilayers [Figure 2 (middle and bottom rows)], the 14-mer peptide seems to perturb the lipid orientation in a similar manner.

In the perpendicular orientation, i.e., with the bilayer normal perpendicular to the magnetic field direction, ^{2}H NMR spectra are mainly sensitive to motional disorder. In the DMPC system [Figure 3A (bottom row)], when the bilayers are in the perpendicular orientation, a slight increase is observed in the quadrupolar splitting of the plateau region of lipid acyl chains in the presence of the 14-mer peptide. Similar results have also been obtained by Mani et al. with PG-1 peptide in POPC/POPG bilayers (*40*). For the DPPC system in the perpendicular orientation, however [Figure 3B (bottom row)], there is a decrease in the quadrupolar splitting of both the plateau and the methyl region of the lipid acyl chains. Because no powder pattern is observed at ±5 kHz on the DMPC and DPPC ^{2}H NMR spectra in the perpendicular orientation, we can conclude that the presence of a powder pattern in the parallel orientation results from orientational disorder in DMPC bilayers, whereas both orientational and motional disorders are present in DPPC bilayers upon peptide addition. The ordering effect of the plateau region of DMPC bilayers stacked between glass plates upon the 14-mer peptide addition, as revealed by the increase in $\Delta\nu_P$ and S_{CD} order parameter, is consistent with previous results on DMPC multilamellar vesicles and supports the possible surface location and capping effect of the 14-mer peptide on the lipid molecules (*31*).

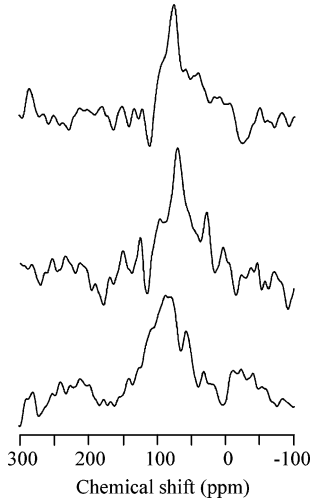

FIGURE 4: ^{15}N NMR spectra of the 14-mer peptide incorporated in mechanically oriented lipid bilayers of DLPC (top row) and DMPC (middle row) at 37 °C and DPPC (bottom row) at 50 °C at a lipid/peptide molar ratio of 60:1.

(C) Nitrogen-15 NMR. We have used proton-decoupled solid-state ^{15}N NMR spectroscopy to investigate the membrane orientation of the 14-mer peptide in DLPC, DMPC, and DPPC bilayers stacked between glass plates. This can be done using a ^{15}N-labeled peptide incorporated into oriented bilayers due to the orientational dependence of the ^{15}N chemical shift. The 14-mer peptide has been synthesized with ^{15}N incorporated into the leucine residue at position 4 in the amino acid sequence (Figure 1). Due to the helical conformation of the 14-mer peptide, and to the size and orientation of the σ_{33} element of the ^{15}N chemical shift tensor, it is possible to correlate the ^{15}N chemical shift with the helix orientation relative to the magnetic field direction from oriented ^{15}N NMR spectra (*41*, *42*). Chemical shifts below 100 ppm or higher than 200 ppm are expected for helical peptides oriented in an in-plane or transmembrane fashion, respectively.

The ^{15}N NMR spectra of the 14-mer peptide incorporated in mechanically aligned bilayers are displayed in Figure 4. The common feature to the three peptide-containing bilayers is the presence of one resonance at a chemical shift below 100 ppm. The peaks are observed at 75.0, 70.0, and 84.0 ppm for DLPC (top row), DMPC (middle row), and DPPC bilayers (bottom row). These chemical shifts correspond to a surface orientation for the 14-mer peptide, regardless of the bilayer hydrophobic thickness. Intensity in the 25−60 ppm range is in part due to the natural abundance of ^{15}N of the lipid choline headgroup.

Numerous membrane-active peptides have been reported to have a surface orientation (*43*−*45*). Chemical shifts of 75 and 70 ppm obtained for the 14-mer peptide in DLPC and DMPC bilayers correspond to the upfield end of the ^{15}N chemical shift powder pattern, whereas the chemical shift of 84 ppm obtained in DPPC bilayers slightly deviates from this value. The deviation in DPPC bilayers could be explained by a slight tilt of the peptide relative to the magnetic field direction or motion of the peptide that narrows the powder pattern (*46*). Also, the ^{15}N resonance observed for the 14-mer peptide in DPPC bilayers appears to be broadened compared to the ^{15}N resonances obtained for the 14-mer peptide in DLPC and DMPC bilayers. This broadening of the resonance for the 14-mer peptide incorporated in DPPC bilayers could be explained by a larger heterogeneity in the membrane orientation of the peptide, compared to its orientation in DLPC and DMPC bilayers. It could also be explained by membrane surface defects since the ^{31}P NMR spectra of DPPC/14-mer bilayers showed a greater membrane disorder alignment with a loss of bilayer alignment of 33%. Mattila et al. have studied the first internal S4 segment of voltage-gated sodium channels in POPC and POPC/POPS bilayers (*47*). They have observed that, despite the fact that the peptide is oriented on the bilayer surface in both systems, the ^{15}N NMR resonance is broadened in POPC/POPS bilayers compared to that in POPC bilayers. They have proposed that the broadening can be due to conformational and topological fluctuations of the peptide, as well as membrane defects such as bilayer undulations and misalignments. Sudheendra et al. have also reported similar behavior of the model ion channel peptide in DOTAP lipid bilayers at high peptide concentration, where they correlated the increase dispersion of the ^{15}N NMR signal to membrane distortions or misalignments and/or to peptide conformational changes (*48*). From the ^{15}N NMR spectra obtained in the present study, it seems that the 14-mer peptide adopts a homogeneous topology in DLPC and DMPC bilayers, whereas it adopts a broader range of surface orientations with slight tilts and/or conformational changes in DPPC bilayers. The possible heterogeneity in the membrane topology of the 14-mer peptide in DPPC bilayers seems to be correlated to its disordering effect in the DPPC acyl chains as revealed by ^{2}H NMR spectroscopy (Figure 3B).

(D) Distance Measurement. We have also investigated the location of the 14-mer peptide in DMPC lipid bilayers by the REDOR technique. More specifically, $^{15}N\{^{31}P\}$ REDOR allows the measurement of intermolecular dipole−dipole interactions between the [^{15}N]leucine residue in the 14-mer peptide and the ^{31}P nucleus in the phospholipid headgroup. The determination of the relative position of the 14-mer peptide with respect to the polar headgroups has been performed on lyophilized DMPC multilamellar vesicles at ∼−10 °C to minimize all large-amplitude motions. Figure 5 shows the $^{15}N\{^{31}P\}$ REDOR dephasing $\Delta S/S_0$ curve for the [^{15}N]Leu_4-14-mer peptide as a function of the dipolar evolution time for a lipid/peptide molar ratio of 60:1.

By fitting the experimental points corresponding to the dipolar evolution time range from 0 to 35 ms, a mean distance of 7.6 ± 0.6 Å seems to dominate the dephasing up to 35 ms of dipolar evolution time. The dephasing did not extend over 35 ms possibly because of the low signal-to-noise-ratio, the small size of the dipolar coupling, or spin−spin relaxation. Toke et al. have performed a similar study with an analogue of the magainin family, the K3 peptide, in interaction with lyophilized MLVs, and they measured a ^{15}N-$\{^{31}P\}$ distance of 5.2 Å (*49*). Hirsh et al. have performed $^{13}C\{^{31}P\}$ REDOR experiments by measuring intermolecular distances between ^{13}C-labeled magainin analogue peptides and the lipid headgroup, in a similar manner to the $^{15}N\{^{31}P\}$ REDOR approach (*50*). The distance range they measured is similar to the one we obtained and supports a model where the peptide is bound near the phospholipid headgroups.

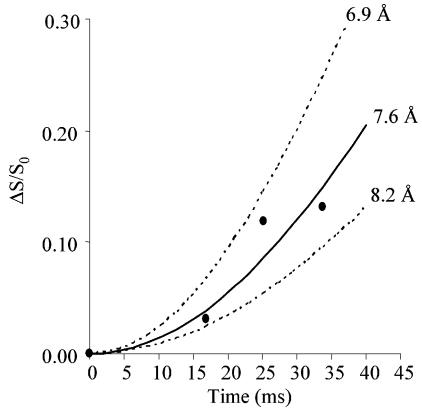

FIGURE 5: 40.5 MHz $^{15}N\{^{31}P\}$ REDOR dephasing ($\Delta S/S_0$) for the 14-mer peptide in lyophilized DMPC multilamellar vesicles at a lipid/peptide molar ratio of 60:1. The spinning speed was 3800 Hz. The solid line is the best fit to the experimental $\Delta S/S_0$ values and corresponds to a mean internuclear $^{15}N-^{31}P$ distance of 7.6 ± 0.6 Å. The dotted lines illustrate the distribution of distances.

Mechanism of Membrane Perturbation. The goal of the present study was to determine the membrane topology of the 14-mer peptide to shed light on its mechanism of membrane perturbation. Solid-state NMR spectroscopy has been shown to be very useful to probe the interactions and the membrane topology of the 14-mer peptide in DLPC, DMPC, and DPPC bilayers stacked between glass plates. Our ^{31}P, ^{2}H, ^{15}N, and REDOR NMR results suggest that the 14-mer peptide perturbs the lipid bilayer integrity. We can obviously rule out the barrel-stave and detergent-like mechanisms, since no resonance has been observed in the downfield region of the ^{15}N chemical shift powder pattern in all bilayers, as well as the absence of an isotropic resonance in all NMR spectra. With the peptide concentration for which the membrane activity of the 14-mer peptide has been observed in previous and present studies, the carpet-like model is very unlikely. In fact, supposing that all of the peptide is bound to the bilayer, we evaluate that there are at maximum 17 peptide molecules per thousand lipid molecules. As reported by Wieprecht et al., who studied model peptides of various polar angles, membrane permeabilization that occurs in such range of peptide concentration is much lower than the required concentration to form a carpet leading to membrane disintegration (*51*).

Previous fluorescent spectrometric results reported that the dye leakage of vesicles is inhibited by the presence of POPE lipids added to PC and slightly increased by the addition of LPC (*30*). We can explain these observations by the fact that the inverse-cone shapes of LPC and the 14-mer peptide are agonistic and both contribute to the induction of a positive bilayer curvature and then increase the dye leakage (Figure 6). The positive curvature strain imposed on the bilayer by

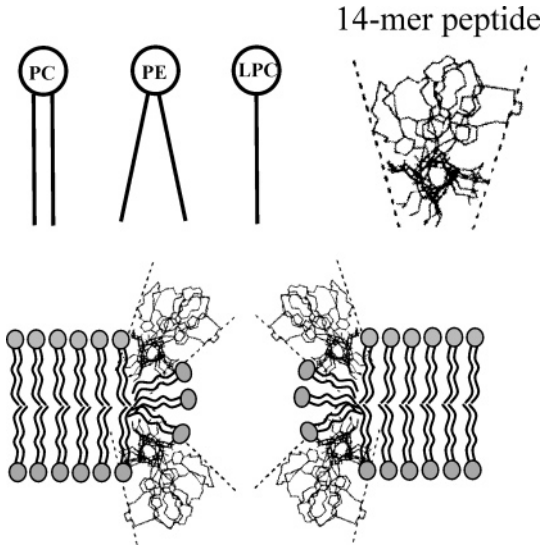

FIGURE 6: Cross-sectional views of (A) cylindrical PC, (B) cone-shaped PE, (C) inverse-cone-shaped LPC, (D) inverse-cone-shaped 14-mer peptide, and (E) the positive curvature strain and membrane destabilization imposed by the 14-mer peptide laid at the bilayer surface (adapted from ref *30* and reproduced with permission of The Royal Society of Chemistry).

the peptide is, however, counterbalanced by the presence of the cone-shaped POPE lipids that have an antagonistic shape compared to the shape of the 14-mer peptide. When the bilayer undergoes a positive curvature strain, the lipid molecules that surround the peptide are constrained to tilt relative to the bilayer normal. These lipids could then contribute to the powder pattern signal observed in both ^{31}P and ^{2}H NMR spectra. Because it is reported in the literature that some membrane-active peptides, such as alamethicin, magainin, and melittin, have different membrane topologies depending on their concentration, we have performed ^{31}P, ^{2}H, and ^{15}N NMR experiments on the 14-mer peptide/DMPC system at a lipid/peptide molar ratio of 20:1. As shown in Figure 7, the ^{15}N NMR spectrum (bottom row) indicates that the 14-mer peptide remains at the bilayer surface with a ^{15}N chemical shift of 81.0 ppm, even at a lipid/peptide molar ratio of 20:1. In addition, there is no presence of an additional isotropic phase on ^{31}P and ^{2}H NMR spectra (top and middle rows), reflecting the absence of smaller lipid structures despite the increase in peptide concentration. ^{31}P and ^{2}H NMR spectra only show an increase in orientational disorder compared to that observed at a lipid/peptide molar ratio of 60:1. The results obtained in the present study are complementary to the previous fluorescence results and support a mechanism of membrane perturbation in which the 14-mer peptide binds to the membrane surface, thereby causing local destabilization of the bilayer via positive curvature strain, similar to the in-plane diffusion or toroidal models (Figure 6).

We do not, however, exclude the possible formation of a pore via the toroidal model, since the peptide/lipid complex involved in such a pore imparts the positive curvature strain to the bilayer. Many research groups have already reported the toroidal model for a great variety of natural and synthetic peptides derived from the magainin family and that showed a surface orientation, namely, MSI-843, MSI-78, and magainin 2 (*52*−*54*). The toroidal model could be a possible way to understand the membrane permeabilization activity

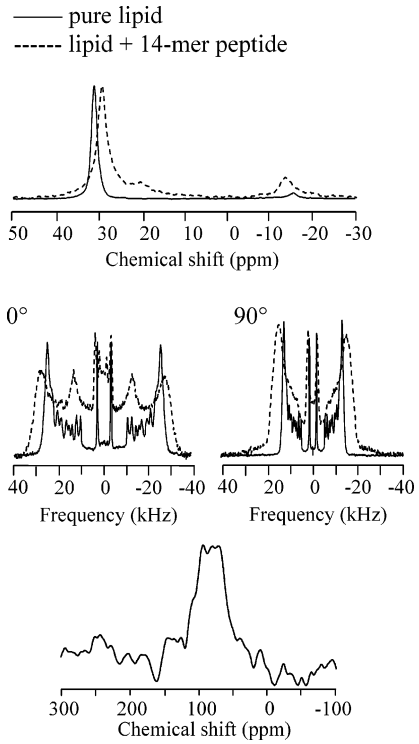

FIGURE 7: ^{31}P (top row) and ^{2}H (middle row) NMR spectra of DMPC mechanically oriented lipid bilayers in the absence and presence of the 14-mer peptide and ^{15}N (bottom row) NMR spectra of the 14-mer peptide incorporated in DMPC mechanically oriented lipid bilayers. The spectra were acquired at 37 °C and at a lipid/peptide molar ratio of 20:1.

of the 14-mer peptide if we consider its shape and the important size of the hydrophilic side composed of crown ethers. We evaluate the polar angle subtended by the crown ethers of the 14-mer peptide to approximately 110°. Uematsu et al. have studied model peptides with polar angles of 100° and 180°, respectively (*55*). They concluded that the peptides with a polar angle of 100° exhibited higher membrane permeabilization activity and pore rate formation. This higher pore rate formation, and therefore the reduced stability of such lipid/peptide complex, could explain the fact that no ^{15}N NMR signal was observed in the chemical shift region characteristic of transmembrane alignment. It is also possible that the number of peptide molecules that contributed to the pore formation is too small to be detected, as suggested for magainin 2 (*56*).

CONCLUSIONS

We have investigated in the present study the membrane topology of a 14-mer amphipathic peptide in oriented model membranes by solid-state NMR spectroscopy. The model membranes used are DLPC, DMPC, and DPPC oriented bilayers stacked between glass plates and lyophilized DMPC multilamellar vesicles. The results obtained from the peptide-containing bilayers stacked between glass plates suggest that the peptide adopts an in-plane orientation and perturbs the membrane via the induction of a positive curvature strain. The membrane topology of the 14-mer peptide in DLPC and DMPC bilayers seems to be homogeneous, whereas the peptide appears to be more deeply inserted in DPPC bilayers, as revealed by the disorder induced in the DPPC headgroup and acyl chains seen in ^{31}P and ^{2}H NMR spectra. The

REDOR experiment performed on lyophilized DMPC multilamellar vesicles also confirms the proximity of the 14-mer peptide to the lipid headgroups.

ACKNOWLEDGMENT

The authors thank Pierre Audet for technical assistance and helpful discussions.

REFERENCES

1. Schmidt, F. R. (2004) The challenge of multidrug resistance: actual strategies in the development of novel antibacterials, *Appl. Microbiol. Biotechnol. 63*, 335−343.
2. Epand, R. M., and Vogel, H. J. (1999) Diversity of antimicrobial peptides and their mechanisms of action, *Biochim. Biophys. Acta 1462*, 11−28.
3. Reddy, K. V. R., Yedery, R. D., and Aranha, C. (2004) Antimicrobial peptides: premises and promises, *Int. J. Antimicrob. Agents 24*, 536−547.
4. Dathe, M., and Wieprecht, T. (1999) Structural features of helical antimicrobial peptides: their potential to modulate activity on model membranes and biological cells, *Biochim. Biophys. Acta 1462*, 71−87.
5. Hancock, R. E. W., and Patrzykat, A. (2002) Clinical development of cationic antimicrobial peptides: from natural to novel antibiotics, *Curr. Drug Targets 2*, 79−83.
6. Marr, A. K., Gooderham, W. J., and Hancock, R. E. W. (2006) Antibacterial peptides for therapeutic use: obstacles and realistic outlook, *Curr. Opin. Pharmacol. 6*, 468−472.
7. Jenssen, H., Hamill, P., and Hancock, R. E. W. (2006) Peptide antimicrobial agents, *Clin. Microbiol. Rev. 19*, 491−511.
8. Strandberg, E., and Ulrich, A. S. (2004) NMR methods for studying membrane-active antimicrobial peptides, *Concepts Magn. Reson. 23A*, 89−120.
9. Hancock, R. E. W., and Chapple, D. S. (1999) Peptide antibiotics, *Antimicrob. Agents Chemother. 43*, 1317−1323.
10. Aisenbrey, C., Kinder, R., Goormaghtigh, E., Ruysschaert, J.-M., and Bechinger, B. (2006) Interactions involved in the realignment of membrane-associated helices. An investigation using oriented solid-state NMR and attenuated total reflection Fourier transform infrared spectroscopies, *J. Biol. Chem. 281*, 7708−7716.
11. Vogt, B., Ducarme, P., Schinzel, S., Brasseur, R., and Bechinger, B. (2000) The topology of lysine-containing amphipathic peptides in bilayers by circular dichroism, solid-state NMR, and molecular modeling, *Biophys. J. 79*, 2644−2656.
12. Harzer, U., and Bechinger, B. (2000) Alignment of lysine-anchored membrane peptides under conditions of hydrophobic mismatch: a CD, ^{15}N and ^{31}P solid-state NMR spectroscopy investigation, *Biochemistry 39*, 13106−13114.
13. Bechinger, B. (1999) The structure, dynamics and orientation of antimicrobial peptides in membranes by multidimensional solid-state NMR spectroscopy, *Biochim. Biophys. Acta 1462*, 157−183.
14. Shai, Y. (2002) Mode of action of membrane active antimicrobial peptides, *Biopolymers 66*, 236−248.
15. Killian, J. A. (1998) Hydrophobic mismatch between proteins and lipids in membranes, *Biochim. Biophys. Acta 1376*, 401−416.
16. Dathe, M., Nikolenko, H., Meyer, J., Beyermann, M., and Bienert, M. (2001) Optimization of the antimicrobial activity of magainin peptides by modification of charge, *FEBS Lett. 501*, 146−150.
17. Bechinger, B., Kinder, R., Helmle, M., Vogt, T. C. B., Harzer, U., and Schinzel, S. (1999) Peptide structural analysis by solid-state NMR spectroscopy, *Biopolymers 51*, 174−190.
18. Fu, R., and Cross, T. A. (1999) Solid-state nuclear magnetic resonance investigation of protein and polypeptide structure, *Annu. Rev. Biophys. Biomol. Struct. 28*, 235−268.
19. Bechinger, B., Aisenbrey, C., and Bertani, P. (2004) The alignment, structure and dynamics of membrane-associated polypeptides by solid-state NMR spectroscopy, *Biochim. Biophys. Acta 1666*, 190−204.
20. Bak, M., Bywater, R. P., Hohwy, M., Thomsen, J. K., Adelhorst, K., Jakobsen, H. J., Sorensen, O. W., and Nielsen, N. C. (2001) Conformation of alamethicin in oriented phospholipid bilayers determined by ^{15}N solid-state nuclear magnetic resonance, *Biophys. J. 81*, 1684−1698.
21. Bechinger, B., Zasloff, M., and Opella, S. J. (1998) Structure and dynamics of the antibiotic peptide PGLa in membranes by solution and solid-state nuclear magnetic resonance spectroscopy, *Biophys. J. 74*, 981−987.
22. Hallock, K. J., Lee, D.-K., and Ramamoorthy, A. (2003) MSI-78, an analogue of the magainin antimicrobial peptides, disrupts lipid bilayer structure via positive curvature strain, *Biophys. J. 84*, 3052−3060.
23. Mecke, A., Lee, D.-K., Ramamoorthy, A., Orr, B. G., and Banaszak Holl, M. M. (2005) Membrane thinning due to antimicrobial peptide binding: an atomic force microscopy study of MSI-78 in lipid bilayers, *Biophys. J. 89*, 4043−4050.
24. Degrado, W. F., and Kaiser, E. T. (1980) Polymer-bound oxime esters as supports for solid-phase peptide synthesis. Preparation of protected peptide fragments, *J. Org. Chem. 45*, 1295−1300.
25. Biron, E., Otis, F., Meillon, J.-C., Robitaille, M., Lamothe, J., Van Hove, P., Cormier, M.-E., and Voyer, N. (2004) Design, synthesis, and characterization of peptide nanostructures having ion channel activity, *Bioorg. Med. Chem. 12*, 1279−1290.
26. Bennett, A. E., Rienstra, C. M., Auger, M., Lakshmi, K. V., and Griffin, R. G. (1995) Heteronuclear decoupling in rotating solids, *J. Chem. Phys. 103*, 6951−6958.
27. Davis, J. H., Jeffrey, K. R., Bloom, M., Valic, M. I., and Higgs, T. P. (1976) Quadrupolar echo deuteron magnetic resonance spectroscopy in ordered hydrocarbon chains, *Chem. Phys. Lett. 42*, 390−394.
28. Mueller, K. T. (1995) Analytic solutions for the time evolution of dipolar-dephasing NMR signals, *J. Magn. Reson. 113A*, 81−93.
29. Gullion, T. (1998) Introduction to rotational-echo double-resonance NMR, *Concepts Magn. Reson. 10*, 277−289.
30. Vandenburg, Y. R., Smith, B. D., Biron, E., and Voyer, N. (2002) Membrane disruption ability of facially amphiphilic helical peptides, *Chem. Commun. 16*, 1694−1695.
31. Ouellet, M., Bernard, G., Voyer, N., and Auger, M. (2006) Insights on the interactions of synthetic amphipathic peptides with model membranes as revealed by ^{31}P and ^{2}H solid-state NMR and infrared spectroscopies, *Biophys. J. 90*, 4071−4084.
32. Seelig, J., and Seelig, A. (1980) Lipid conformation in model membranes and biological membranes, *Q. Rev. Biophys. 13*, 19−61.
33. Seelig, J. (1978) ^{31}P nuclear magnetic resonance and the head group structure of phospholipids in membranes, *Biochim. Biophys. Acta 515*, 105−140.
34. Smith, I. C. P., and Ekiel, I. H. (1984) in *Phosphorus-31 NMR: Principles and Applications* (Gorenstein, D. G., Ed.) pp 447−475, Academic Press, London.
35. Petrache, H. I., Dodd, S. W., and Brown, M. F. (2000) Area per lipid and acyl length distributions in fluid phosphatidylcholines determined by ^{2}H NMR spectroscopy, *Biophys. J. 79*, 3172−3192.
36. Buffy, J. J., McCormick, M. J., Wi, S., Waring, A., Lehrer, R. I., and Hong, M. (2004) Solid-state NMR investigation of the selective perturbation of lipid bilayers by the cyclic antimicrobial peptide RTD-1, *Biochemistry 43*, 9800−9812.
37. Picard, F., Pézolet, M., Bougis, P. E., and Auger, M. (2000) Hydrophobic and electrostatic cardiotoxin-phospholipid interactions as seen by solid-state ^{31}P NMR spectroscopy, *Can. J. Anal. Sci. Spectrosc. 45*, 72−83.
38. Mani, R., Waring, A. J., Lehrer, R. I., and Hong, M. (2005) Membrane-disruptive abilities of β-hairpin antimicrobial peptides correlate with conformation and activity: a ^{31}P and ^{1}H NMR study, *Biochim. Biophys. Acta 1716*, 11−18.
39. Yamaguchi, S., Hong, T., Waring, A., Lehrer, R. I., and Hong, M. (2002) Solid-state NMR investigations of peptide-lipid interaction and orientation of a β-sheet antimicrobial peptide, protegrin, *Biochemistry 41*, 9852−9862.
40. Mani, R., Buffy, J. J., Waring, A., Lehrer, R. I., and Hong, M. (2004) Solid-state NMR investigation of the selective disruption of lipid membranes by protegrin-1, *Biochemistry 43*, 13839−13848.
41. Bechinger, B., and Sizun, C. (2003) Alignment and structural analysis of membrane polypeptides by ^{15}N and ^{31}P solid-state NMR spectroscopy, *Concepts Magn. Reson. 18A*, 130−145.
42. Bechinger, B. (2000) Biophysical investigations of membrane perturbations by polypeptides using solid-state NMR spectroscopy, *Mol. Membr. Biol. 17*, 135−142.
43. Porcelli, F., Buck, B., Lee, D.-K., Hallock, K. J., Ramamoorthy, A., and Veglia, G. (2004) Structure and orientation of pardaxin determined by NMR experiments in model membranes, *J. Biol. Chem. 279*, 45815−45823.

44. Bechinger, B., Zasloff, M., and Opella, S. J. (1993) Structure and orientation of the antibiotic peptide magainin in membranes by solid-state nuclear magnetic resonance spectroscopy, *Protein Sci. 2*, 2077−2084.
45. Marassi, F. M., Opella, S. J., Juvvadi, P., and Merrifield, R. B. (1999) Orientation of cecropin A helices in phospholipid bilayers determined by solid-state NMR spectroscopy, *Biophys. J. 77*, 3152−3155.
46. Henzler Wildman, K. A., Lee, D.-K., and Ramamoorthy, A. (2003) Mechanism of lipid bilayer disruption by the human antimicrobial peptide, LL-37, *Biochemistry 42*, 6545−6558.
47. Mattila, K., Kinder, R., and Bechinger, B. (1999) The alignment of a voltage-sensing peptide in dodecylphosphocholine micelles and in oriented lipid bilayers by nuclear magnetic resonance and molecular modeling, *Biophys. J. 77*, 2102−2113.
48. Sudheendra, U. S., and Bechinger, B. (2005) Topological equilibria of ion channel peptides in oriented lipid bilayers revealed by ^{15}N solid-state NMR spectroscopy, *Biochemistry 44*, 12120−12127.
49. Toke, O., Maloy, W. L., Kim, S. J., Blazyk, J., and Schaefer, J. (2004) Secondary structure and lipid contact of a peptide antibiotic in phospholipid bilayers by REDOR, *Biophys. J. 87*, 662−674.
50. Hirsh, D. J., Hammer, J., Maloy, W. L., Blazyk, J., and Schaefer, J. (1996) Secondary structure and location of a magainin analogue in synthetic phospholipid bilayers, *Biochemistry 35*, 12733−12741.
51. Wieprecht, T., Dathe, M., Epand, R. M., Beyermann, M., Krause, E., Maloy, W. L., MacDonald, D. L., and Bienert, M. (1997) Influence of the angle subtended by the positively charged helix face on the membrane activity of amphipathic, antibacterial peptides, *Biochemistry 36*, 12869−12880.
52. Matsuzaki, K., Sugishita, K.-i., Ishibe, N., Ueha, M., Nakata, S., Miyajima, K., and Epand, R. M. (1998) Relationship of membrane curvature to the formation of pores by magainin 2, *Biochemistry 37*, 11856−11863.
53. Ramamoorthy, A., Thennarasu, S., Lee, D.-K., Tan, A., and Maloy, L. (2006) Solid-state NMR investigation of the membrane-disrupting mechanism of antimicrobial peptides MSI-78 and MSI-594 derived from magainin 2 and melittin, *Biophys. J. 91*, 206−216.
54. Thennarasu, S., Lee, D.-K., Tan, A., Kari, P., and Ramamoorthy, A. (2005) Antimicrobial activity and membrane selective interactions of a synthetic lipopeptide MSI-843, *Biochim. Biophys. Acta 1711*, 49−58.
55. Uematsu, N., and Matsuzaki, K. (2000) Polar angle as a determinant of amphipathic a-helix-lipid interactions: a model peptide study, *Biophys. J. 79*, 2075−2083.
56. Matsuzaki, K. (1998) Magainins as paradigm for the mode of action of pore forming polypeptides, *Biochim. Biophys. Acta 1376*, 391−400.

BI0620151